

## THE FATE OF SPIRAL GALAXIES IN CLUSTERS: THE STAR FORMATION HISTORY OF THE ANEMIC VIRGO CLUSTER GALAXY NGC 4569.

A. BOSELLI<sup>1</sup>, S. BOISSIER<sup>1,2</sup>, L. CORTESE<sup>1,6</sup>, A. GIL DE PAZ<sup>2,3</sup>, M. SEIBERT<sup>4</sup>, B. F. MADORE<sup>2,5</sup>, V. BUAT<sup>1</sup>, D. C. MARTIN<sup>4</sup>  
*Draft version October 8, 2018*

### ABSTRACT

We present a new method for studying the star formation history of late-type, cluster galaxies undergoing gas starvation or a ram-pressure stripping event by combining bidimensional multifrequency observations with multi-zones models of galactic chemical and spectrophotometric evolution. This method is applied to the Virgo cluster anemic galaxy NGC 4569. We extract radial profiles from recently obtained UV GALEX images at 1530 and 2310 Å, from visible and near-IR narrow (H $\alpha$ ) and broad band images at different wavelengths ( $u$ , B,  $g$ , V,  $r$ ,  $i$ ,  $z$ , J, H, K), from Spitzer IRAC and MIPS images and from atomic and molecular gas maps. The model in the absence of interaction (characterized by its rotation velocity and spin parameter) is constrained by the unperturbed H band light profile and by the H $\alpha$  rotation curve. We can reconstruct the observed total-gas radial-density profile and the light surface-brightness profiles at all wavelengths in a ram-pressure stripping scenario by making simple assumptions about the gas removal process and the orbit of NGC 4569 inside the cluster. The observed profiles cannot be reproduced by simply stopping gas infall, thus mimicing starvation. Gas removal is required, which is more efficient in the outer disk, inducing a radial quenching in the star formation activity, as observed and reproduced by the model. This observational result, consistent with theoretical predictions that a galaxy-cluster IGM interaction is able to modify structural disk parameters without gravitational perturbations, is discussed in the framework of the origin of lenticulars in clusters.

*Subject headings:* Galaxies: individual: (NGC 4569-M90) – Galaxies: interactions – Ultraviolet: galaxies – Galaxies: clusters: individual: Virgo

### 1. INTRODUCTION

Perturbations induced by the harsh cluster environment makes the evolution of cluster galaxies different than that of their counterparts in the field. Besides the well known morphology segregation effect (Dressler 1980; Whitmore et al. 1993), there is also evidence clearly indicating that the cluster late-type galaxy population is systematically different from the field: cluster spirals are generally depleted in their total HI content and are less active in forming stars than their isolated counterparts. This is most recently and extensively reviewed in Boselli & Gavazzi (2006). The nature of the perturbing phenomenon has not yet been unambiguously identified. Several physical processes have been proposed to explain gas removal in clusters. Some of them are related to the dynamical interactions of cluster galaxies with the hot ( $T_{IGM} \sim 10^7$  K) and dense ( $\rho_{IGM} \sim 10^{-3}$  atom cm<sup>-3</sup>) intergalactic medium (IGM) (ram-pressure, Gunn & Gott 1972; viscous stripping, Nulsen 1982; thermal evaporation, Cowie & Songaila 1977). Others are due to the gravitational interactions with nearby companions

(Merritt 1983) or with the wider potential of the cluster (Byrd & Valtonen 1990). The detailed analysis of several well known resolved galaxies in the Virgo and in the Coma clusters, generally favor a galaxy-IGM interaction scenario (Vollmer et al. 1999, 2000, 2001a, 2004b; Kenney et al. 2004; Yoshida et al. 2004) in these instance. Using complete, multifrequency datasets combined with model predictions several studies have unambiguously shown that ram-pressure stripping occurs even at the periphery of clusters (e.g. CGCG 97-73 and 97-79 in A1367, Gavazzi et al. 2001), and that galaxies recently ( $\leq 500$  Myr) stripped by ram-pressure populate nearby clusters well outside the cluster core (Boselli & Gavazzi 2006).

Ram-pressure stripping has also been invoked to explain the origin of the lenticular galaxy population inhabiting rich clusters. One early suggestion was that, as a consequence of gas removal through ram-pressure stripping, cluster galaxies first become “anemic” and then passively evolved into lenticulars (van den Bergh 1976). Statistical considerations, as well as structural, kinematical and spectroscopic properties of lenticulars, however, do not appear to confirm this simple scenario. As discussed in Dressler (1980, 2004) the morphological type variation in clusters is too weak a function of the local galaxy density. Furthermore, the disks of lenticulars have, on average, surface brightnesses and bulge-to-disk ratios that are significantly higher than early-type spirals (Dressler 1980; Christlein & Zabludoff 2004; Boselli & Gavazzi 2006) making the formation of lenticulars through gas sweeping in spirals very unlikely. The larger scatter and a small zero-point offset in the Tully-Fisher relation observed in the Virgo and Coma

<sup>1</sup> Laboratoire d’Astrophysique de Marseille, BP8, Traverse du Siphon, F-13376 Marseille, France

<sup>2</sup> Observatories of the Carnegie Institution of Washington, 813 Santa Barbara St., Pasadena, CA 91101

<sup>3</sup> Departamento de Astrofísica y CC. de la Atmósfera, Universidad Complutense de Madrid, Avda. de la Complutense, s/n, E-28040 Madrid, Spain

<sup>4</sup> California Institute of Technology, MC 405-47, 1200 East California Boulevard, Pasadena, CA 91125

<sup>5</sup> NASA/IPAC Extragalactic Database, California Institute of Technology, Mail Code 100-22, 770 S. Wilson Ave., Pasadena, CA 91125

<sup>6</sup> School of Physics and Astronomy, Cardiff University, 5, The Parade, Cardiff CF24 3YB, UK

cluster lenticulars also indicate that S0s can hardly be formed by simple gas removal from healthy spirals (Hinz et al. 2003). Furthermore cluster lenticulars generally have spectroscopic signatures of recent, post-starburst activity (Poggianti et al. 2004) difficult to trigger in a simple ram-pressure stripping scenario.

The origin of lenticulars is still an open problem and limit our understanding of the evolution of galaxies in different environments. This riddle can be solved only by first realistically quantifying the physical effects of ram-pressure stripping by combining model predictions with multifrequency observations of representative samples.

We have been collecting multi-frequency data for a large sample of late-type galaxies in nearby clusters and in the field in order to undertake the comparative statistical analysis of any systematic differences between cluster and field objects. The most important results obtained from the analysis done so far are reported in Boselli & Gavazzi (2006). Combined with multi-zone models for the chemical and spectrophotometric evolution of galaxies (Boissier & Prantzos 2000), this unique database is helping us to understand the evolution of cluster spirals. The aim of the present paper is to give a complete description of the multi-zone spectrophotometric models of galaxy evolution used to study the effects of the environment on cluster galaxies.

As a first application we present a detailed study of the radial profiles of the Virgo cluster galaxy NGC 4569 (M90). NGC 4569, the prototype anemic galaxy as defined by van den Bergh (1976), is extremely deficient in HI, having only about one tenth of the atomic gas of a comparable field galaxy of similar type and dimensions. This galaxy has a truncated H $\alpha$  and HI radial-density profile (at a radius of  $\sim 5$  kpc; see Fig. 1 and 3) as firstly noticed by Koopmann & Kenney (2004a,b) and Cayatte et al. (1994), bearing witness to a recent interaction with the cluster environment. NGC 4569 is located close ( $\sim 2$  degrees,  $\sim 240$  kpc for a virial radius of 1.7 Mpc) to the cluster center. Being one of the largest galaxies ( $\sim 10$  arcmin,  $\sim 50$  kpc) in the Virgo cluster, NGC 4569 is the ideal candidate for our study since it is spatially resolved at all the wavelengths considered here. NGC 4569 has also been selected because it has been previously studied using dynamical models by Vollmer et al. (2004a). A direct comparison of the results obtained using totally independent techniques (in particular, dating the interaction) is thus possible. We just remind that multifrequency and kinematical observation of the inner part of NGC 4569 done by Jogee et al. (2005) seem to indicate that the nucleus and the inner stellar bar of the galaxy might have been triggered by a recent tidal interaction. There are however no observational evidences indicating that the HI disk has been truncated by any gravitational interaction with nearby companions. Since our models are adapted for disk galaxies, we will however limit our study to the disk component excluding the central nucleus.

The combination of the multi-frequency 2-D data with our spectrophotometric models allow us to study, for the first time, the radial evolution of the different stellar populations in this prototype, gas-stripped cluster galaxy with the aim of understanding whether its structural

properties can evolve, even in principle, into those of a typical cluster lenticular (S0) galaxy. A more complete analysis of a statistically significant sample of cluster galaxies will be presented in a future communication.

## 2. DATA

The large amount of spectrophotometric data available for NGC 4569, collected in the GOLDMine database (Gavazzi et al. 2003), allow us to reconstruct its radial profile at 22 different wavelengths: from the new GALEX UV bands (at FUV=1530 and NUV=2310 Å, IR1.0 data release recently published in Gil de Paz et al. 2006), to the visible B and V (Boselli et al. 2003), Sloan *u, g, r, i, z* (Abazajian et al. 2005), near-IR J, H and K bands (Boselli et al. 1997; 2MASS Jarrett et al. 2003), mid-IR 3.6, 4.5, 5.8 and 8  $\mu$ m IRAC and far-IR 24, 70 and 160  $\mu$ m MIPS bands recently obtained by Spitzer in the framework of the SINGS project (Kennicutt et al. 2003). An accurate description of the IRAC and MIPS Spitzer data reduction procedures is given in Dale et al. (2005). H $\alpha$ + [NII] narrow band imaging, used to trace the recent star formation activity (e.g. Boselli et al. 2001), is available from Boselli & Gavazzi (2002). Some of the multifrequency images of NGC 4569 are shown in Fig. 1. The accuracy of photometry from the imaging data is, on average about 10%. HI profiles are from Cayatte et al. (1994), while H $_2$  profiles, determined from CO data using a luminosity-dependent CO-to-H $_2$  conversion factor (from Boselli et al. 2002, applied to the whole profile with no radial variation as unfortunately no metallicity gradient information is available for NGC 4569) are taken from the BIMA survey of Helfer et al. (2003) for the inner disk, and from Kenney & Young (1988) for the outer disk. The total gas profile is the sum of the HI and H $_2$  gas profiles multiplied by a factor of 1.4 to take into account the He contribution. The galaxy rotation curve has been taken from Rubin et al. (1999).

The radial surface-density profiles have been constructed by integrating the available images within elliptical, concentric annuli. The ellipticity and position angles have been determined and then fixed using the deepest B-band image following the procedure of Gavazzi et al. (2000)<sup>1</sup>. All the observed profiles have been smoothed to the same angular resolution as the models (which is 1 kpc, see next section). The UV to near-IR broadband radial profiles of the galaxy have been corrected for internal extinction using the recipe of Boissier et al. (2004) based on the radial variation of the far-IR to FUV flux ratio. After masking the contribution of the nucleus, whose emission is contaminated by AGN activity (NGC 4569 is classified as a Seyfert in NED), we combined the 24, 70 and 160  $\mu$ m profiles, smoothed to the 160  $\mu$ m resolution, using the recipe of Dale et al. (2001) to estimate the total 1-1000  $\mu$ m dust emission (TIR) as extensively discussed in Cortese et al. (2006a).

<sup>1</sup> To avoid any possible contamination by the NW arm, whose kinematical properties indicate that it is not associated to the stellar disk but rather formed during the galaxy-cluster IGM interaction, the arm was masked in the construction of the radial profiles. If included, its contribution would be perceptible only in the FUV filter at radii  $> 8$  kpc, increasing the surface brightness by  $< 0.5$  mag.

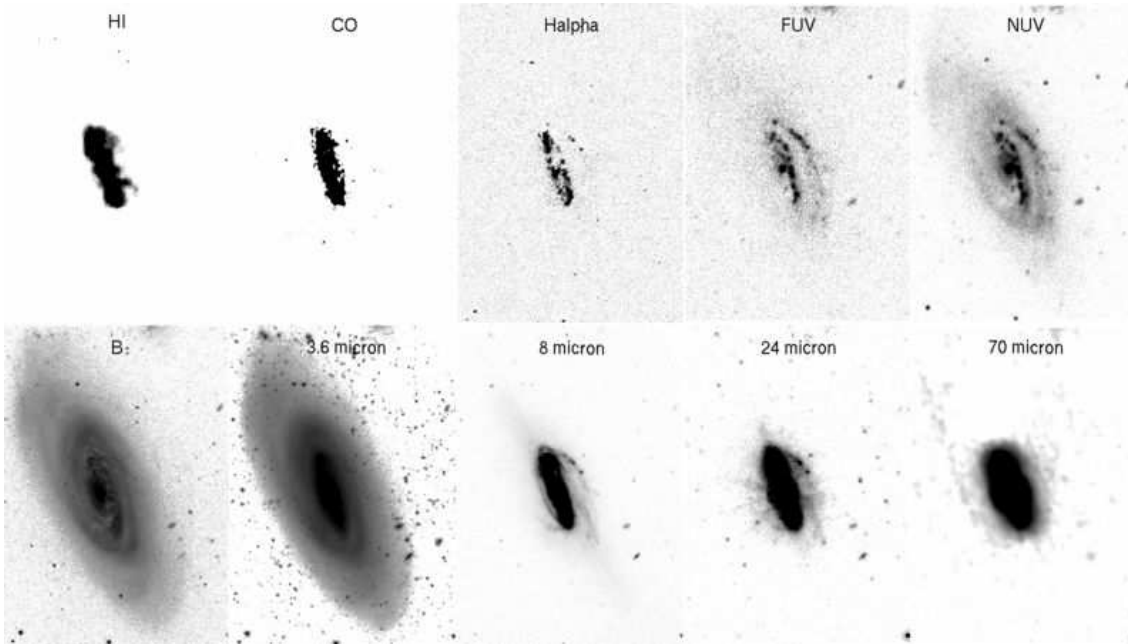


FIG. 1.— The multifrequency images of NGC 4569 at their intrinsic resolution: from top left to bottom right, HI, CO,  $H\alpha$ , FUV, NUV, B, 3.6  $\mu\text{m}$ , 8 $\mu\text{m}$ , 24  $\mu\text{m}$  and 70  $\mu\text{m}$  all on the same scale.

The total far-IR to FUV flux ratio radial variation is then transformed into a FUV extinction gradient (in magnitudes) using the appropriate calibration given in Cortese et al. (in preparation) for a galaxy with spectral properties similar to those of NGC 4569. We stress that, given its quiescent nature, the contribution of far-UV photons to the dust heating of NGC 4569 is only marginal: the calibration of the far-IR to FUV flux ratio into a FUV extinction is thus more indirect than in star forming galaxies, where dust is mostly heated by UV photons, making the correction highly uncertain. The adopted far-IR to FUV flux ratio vs.  $A(\text{FUV})$  relation calibrated on the spectral energy distribution of NGC 4569 allow us to take into account also the contribution to dust heating from the general interstellar radiation field not necessarily associated to star forming regions. Indeed we predict less extinction for the same TIR/FUV ratio than for star forming galaxies (Buat et al. 2005). The extinction in the other visible and near-IR bands has been determined using the prescription of Boselli et al. (2003). The resulting  $A(\text{FUV})$  extinction profile, along with  $A(\text{B})$  and  $A(\text{H})$ , are shown in Fig. 2: given the lack of gas and dust in the outer disk, extinctions are extrapolated to zero at large radii. As extensively discussed in the next sections, the determination of the radially-dependent extinction corrections, that can be quite large (i.e., more than 1 mag) in the UV bands, is thus the major source of systematic uncertainty in the reconstruction of the corrected radial profiles.

$H\alpha + [\text{NII}]$  narrow-band imaging has been corrected for  $[\text{NII}]$  contamination and dust extinction (Balmer decrement) using the integrated spectroscopy of Gavazzi et al. (2004). Given the nature of the integrated spectrum, these corrections are fixed and do not change with radius. We believe that such a constant correction does not introduce systematic errors in the  $H\alpha$  profile determination

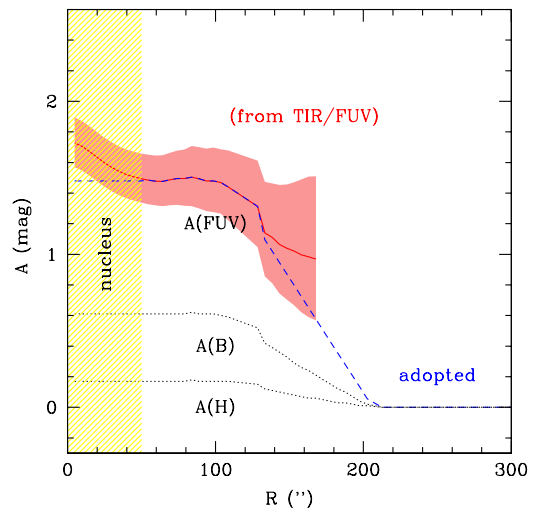


FIG. 2.— The radial variation of the  $A(\text{FUV})$  extinction profile (red solid line) and its uncertainty (red shaded area) as determined from the total far-IR (TIR) to FUV flux ratio. The adopted  $A(\text{FUV})$  extinction correction, determined excluding the contribution of the active nucleus and extrapolating the profile to zero values in the outer disk, is shown by the blue dashed line. The black dotted lines give the extinction profiles in the B and H band.

given the strongly truncated morphology of the galaxy. It is generally considered that radial effects are small for these corrections (e.g., Martin & Kennicutt 2001). On the other hand, the integrated spectrum might be partly contaminated by the nuclear emission (the galaxy is classified as a Seyfert in NED). In any case  $[\text{NII}]$  contamination and extinction are the two major sources of uncertainty in the determination of the  $H\alpha$  radial profile.

In Fig. 3, we show all the gas and stellar profiles described above, at 1 kpc resolution. For the surface photometry, open symbols correspond to observed values, and filled symbols to extinction-corrected values. The shaded area in between the two profiles graphically illustrates the magnitude of the uncertain extinction correction. We notice that, although not univocally related to star formation (Boselli et al. 2004), the unextinguished 8  $\mu\text{m}$  image (Fig. 1) and radial profile (Fig. 4) of NGC 4569 confirm the truncated nature of the star forming disk.

### 3. MODELS

#### 3.1. *The multi-zone models for the chemical and spectro-photometric unperturbed disk evolution*

To study the evolution of the disk of NGC 4569 at various radii, we have used the multi-zone (typical resolution  $\sim 1$  kpc) chemo-spectrophotometric models of Boissier & Prantzos (2000), updated with an empirically-determined star formation law (Boissier et al. 2003) relating the star formation rate to the total-gas surface densities ( $\Sigma_{SFR}$ ,  $\Sigma_{gas}$ ):

$$\Sigma_{SFR} = \alpha \Sigma_{gas}^{1.48} V(R)/R \quad (1)$$

where  $V(R)$  is the rotation velocity at radius  $R$ . The resulting models are extremely similar to those in Boissier & Prantzos (2000) and show the same global trends. Not only do we consider the star formation law as fixed but we also keep the same mass accretion (infall) histories as in Boissier & Prantzos (2000), based on the assumption that before the interaction with the cluster, NGC4569 was a “normal” spiral. The only remaining free parameters in this grid of models are the spin parameter,  $\lambda$  and rotational velocity,  $V_C$ . The spin parameter is a dimensionless measure of the angular momentum (defined in e.g. Mo, Mao & White 1998). Its value in spirals ranges typically between  $\sim 0.02$  for relatively compact galaxies to  $\sim 0.09$  for low surface brightness galaxies (Boissier & Prantzos 2000). The models of Boissier & Prantzos (2000) contains scaling relationships (the total mass varies as  $V_C^3$ , the scale-length as  $\lambda \times V_C$ ). Star formation histories depend on the infall timescales, which are a function of  $V_C$  in these models, so that roughly speaking,  $V_C$  controls the stellar mass accumulated during the history of the galaxy, and  $\lambda$  its radial distribution. To constrain these two parameters, we use the H-band luminosity profile (determined assuming a distance of 17 Mpc) and the rotation curve of the galaxy, making the reasonable assumption that both of these observables are unperturbed during the interaction<sup>2</sup>. Since the model does not include any bulge or nuclear component, throughout the paper the comparison between models and observed profiles is limited to the disk component, excluding the inner  $\sim 40''$  (3 kpc). In order to fix the two parameters, we proceeded as follow: for each spin considered (0.01 to 0.09 in 0.01 steps), we computed models with various rotational velocities (80 to 360, in steps of 70 km s<sup>-1</sup>) and interpolated the models for each spin in

order to find the velocity for which the integrated H band magnitude is equal to the observed one, after 13.5 Gyr of evolution (considered as the present epoch). We then compared the model profile in the H band for each spin (with the velocity determined as described above) to the observed profile. The best agreement was clearly obtained with  $\lambda=0.04$  and the associated  $V_C=270$  km s<sup>-1</sup>. The disk is more concentrated (extended) than observed for smaller (larger) spin parameters. The resulting rise of the rotation curve for this model is consistent with the observed one (see Fig. 5 for a comparison of this model and the constraints mentioned above). The model does not reproduce small scales variations probably due to structures such as spiral arms. Given the agreement, this model will now be considered as the reference model for the unperturbed case. The models of Boissier & Prantzos (2000) provide the luminosity profiles in all bands as well as the total gas profile. They do not compute the nebular emission, but we estimated the H $\alpha$  emission here by using the number of ionizing photons predicted by Version 5 of STARBURST 99 (Vazquez & Leitherer 2005) for a single generation of stars distributed on the Kroupa et al. (1993) initial mass function (as used in our models), convolving it with our star formation history, and converting the result into our H $\alpha$  flux following Appendix A of Gavazzi et al. (2002b). All the profiles predicted for the reference model (without any interaction, solid line) are compared to the observed one in Fig. 3. The profiles at long wavelengths are in agreement with the model, while short-wavelength observations, the star formation tracers (UV, H $\alpha$ ), and the gas profiles present truncations and/or shorter scale-lengths with respect to the expectations of the unperturbed model.

#### 3.2. *The starvation scenario*

In the starvation scenario (Larson et al. 1980, Balogh et al. 2000, Treu et al. 2003), the cluster acts on large scales by removing any extended gaseous halo surrounding the galaxy, preventing further infall of such gas onto the disk. The galaxy then become anemic simply because it exhausts the gas reservoir through on-going star formation.

Infall is a necessary assumption in models of the chemical evolution of the Milky Way to account for the G-dwarf metallicity distribution (Tinsley 1980) and is supported by some chemo-dynamical models (Samland et al. 1997). As the disk galaxy models were obtained through a generalisation of the Milky Way model, infall is present in all our models. It is a schematic but simple way to describe the growth of any galaxy from a proto-galactic clump in the distant past to a massive present-day galaxy. Infall time scales in the models were chosen to reproduce the properties of present day normal galaxies (Boissier & Prantzos 2000, Boissier et al. 2001). A radial variation of infall time-scales is suggested by dynamical models (Larson 1976). A prescription for this variation was implemented in our models of the Milky Way and of spirals, allowing to reproduce many profiles and abundance gradients in our Galaxy (Boissier & Prantzos 1999, Hou et al. 2000), as well as colour and abundance gradients in external galaxies (Prantzos & Boissier 2000).

Stopping infall (in order to mimic starvation) at a given time is straightforward to include in the model. We shall call  $t_s$  the elapsed time since the infall termination (look

<sup>2</sup> The H-band luminosity, proportional to the total dynamical mass of the galaxy (Gavazzi et al. 1996) and tracer of the old stellar population, and the rotational velocity of galaxies are generally not affected by the interaction with the harsh cluster environment (Boselli & Gavazzi 2006).

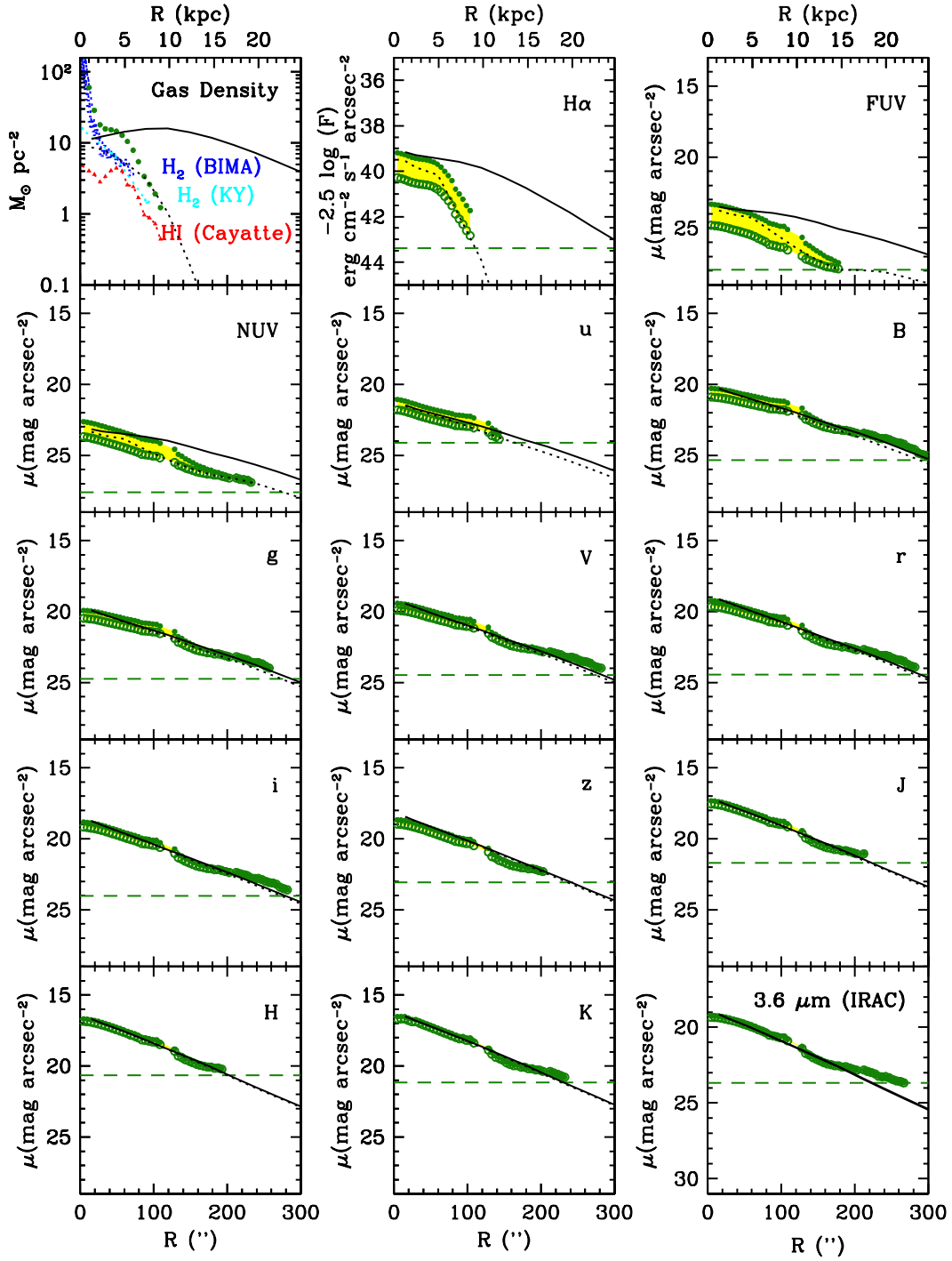


FIG. 3.— Profiles in NGC 4569. For the photometry, the open symbols are the observed values, the filled symbols the ones corrected for extinction. The dashed horizontal line in each panel indicates detection limits, determined as described in Gil de Paz & Madore (2005) for a S/N  $\sim 1$ , where the rms is a combination of the pixel per pixel and large scale sky background rms. The total gas profile (top left panel: filled circles) is computed from the sum of the HI from Cayatte et al. 1994 (filled triangles), H<sub>2</sub> from Helfer et al. 2003 (BIMA) and Kenney & Young 1988 (KY); corrected for a Helium contribution ( $\times 1.4$ ). The observations were smoothed to 1 kpc, matching the resolution used in the models. The solid and dotted lines are respectively the reference model, and our best-model including ram pressure (see text for details on the models).

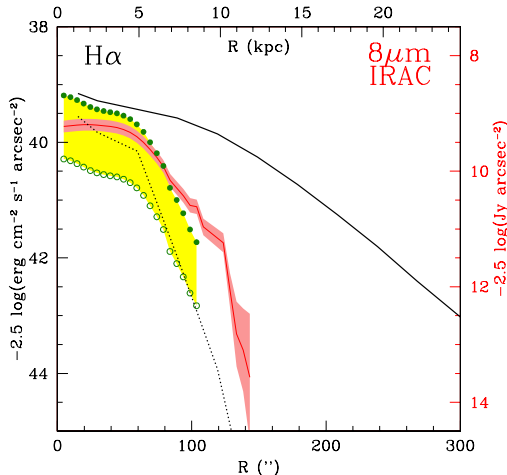


FIG. 4.— The comparison of the observed (green empty circles) and corrected (green filled circles) H $\alpha$  and 8  $\mu\text{m}$  IRAC (red line) radial profiles. Both the H $\alpha$  and the 8  $\mu\text{m}$  IRAC (red line) radial profiles are strongly truncated if compared to the unperturbed model (black solid line), and qualitatively similar to the radial variation of the star formation activity predicted by the adopted perturbed model in a ram pressure scenario (black dotted line).

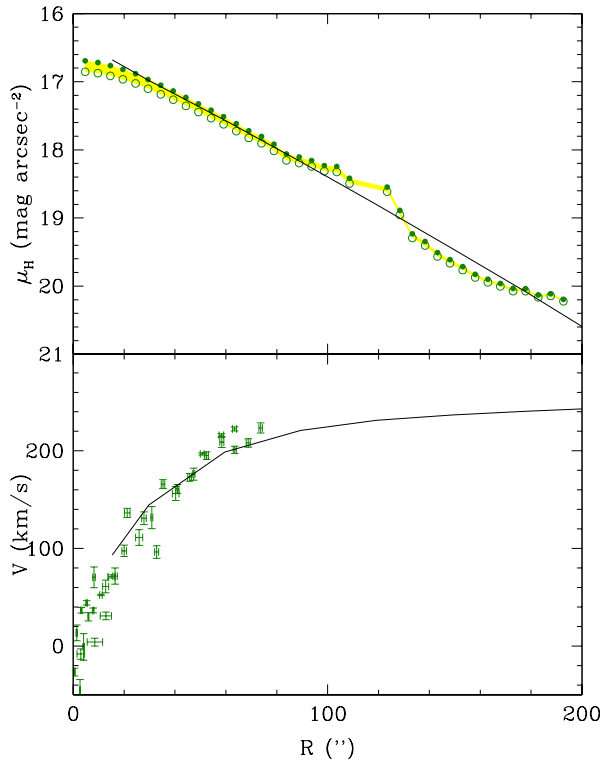


FIG. 5.— The radial profile of observed (open symbols) and extinction-corrected (filled symbols) H-band surface brightness (top) and of the rotational velocity (bottom) used to constrain the model without interaction (represented by the black solid line). The inner 3 kpc (40  $''$ ) are not used to constrain the model.

back time). In order to affect the evolution of the galaxy, starvation must have occurred before most of the gas had been accreted onto the disk. Regions where infall occurs early-on with respect to the starvation epoch will barely be affected, while those where infall occurs late in the history of the galaxy will never be built up. Starvation is a global effect ( $t_s$  has no dependence on radius); however, the infall time-scale increases with radius (inside-out formation of the galaxy). We can therefore expect an effect on the gas and stellar profiles since starvation will affect the outer regions (since these form late in an isolated galaxy model) more than inner regions (which have already formed at earlier times).

### 3.3. The ram pressure stripping scenario

In addition to the starvation scenario we can also study the effect of ram-pressure gas stripping. For simplicity, we adopt the plausible scenario of Vollmer et al. (2001b) explicitly tailored to Virgo: i.e., the galaxy being modelled has crossed the dense IGM only once, on an elliptical orbit. The ram pressure exerted by the IGM on the galaxy ISM varies in time following a gaussian profile, whose peak at ( $t=t_{rp}$ ) is when the galaxy is crossing the dense cluster core at high velocity ( $t$  and  $t_{rp}$  are look-back times, where the present epoch corresponds to  $t=0$ ). The gaussian has a width  $\Delta t = 9 \times 10^7$  years (see Fig. 3 of Vollmer et al. 2001b). We make the hypothesis that the gas is removed at a rate that is directly proportional to the galaxy gas column density  $\Sigma_{gas}$  and inversely proportional to the potential of the galaxy, measured by the total (baryonic) local density  $\Sigma_{potential}$  (provided by the model). The gas-loss rate adopted is then equal to  $\epsilon \frac{\Sigma_{gas}}{\Sigma_{potential}}$ , with the efficiency  $\epsilon$  following a gaussian having a maximum  $\epsilon_0$  at the time  $t_{rp}$ , chosen to mimic the variation of the ram pressure suggested by Vollmer et al. (2001b). This very simple, but physically-motivated prescription should allow us to model the gas removal from the galaxy using only two free parameters ( $t_{rp}$  and  $\epsilon_0$ ) to age-date and measure the magnitude of this effect. We make the further assumption that no extra star formation is induced during the interaction. This assumption is reasonable since both models (Fujita 1998, Fujita & Nagashima 1999) and observations (Iglesias-Paramo et al. 2004) do not show any significant increase of the star formation activity in galaxies thought to be currently undergoing a ram-pressure stripping event.

## 4. THE STAR FORMATION HISTORY OF NGC 4569: MODEL PREDICTIONS

### 4.1. The starvation scenario

The result of starvation on the gas and star forming (H $\alpha$  and FUV) profiles, once gas infall on the galaxy has been stopped at different epochs ( $t_s$ ), is shown in Fig. 6. First, we note that in order to remove significant amounts of gas in N4569, infall must have been stopped for many Gyr. This is consistent with Balogh et al. (2000). The reason for this is that with  $V_C=270$  km s $^{-1}$ , the reference model has a higher mass than the Milky Way. Since infall timescales in the models of Boissier & Prantzos (2000) are shorter for more massive galaxies, NGC4569 should have accreted most of its material early-on in its history, thus stopping infall at a later time has no effect, as most of the gas is

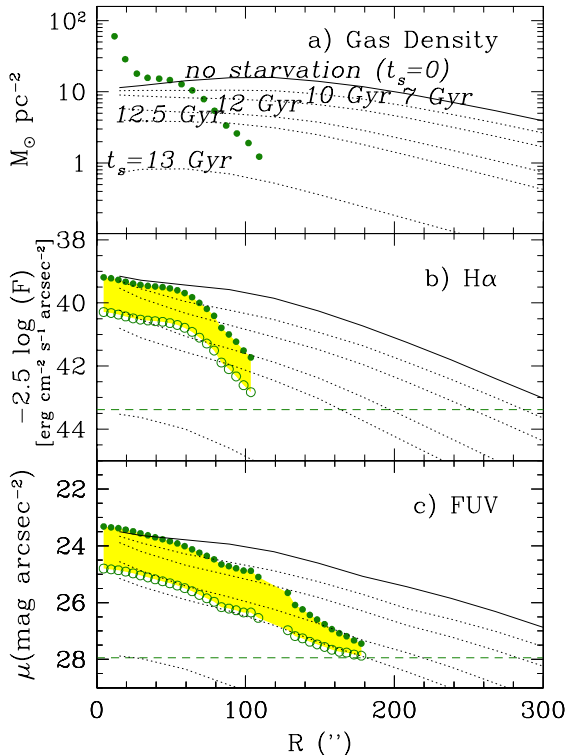


FIG. 6.— The observed (empty circles) and corrected (filled circles) a) gas, b)  $H\alpha$  and c) FUV profiles are compared to the predictions for the reference model (solid line) and starvation models (in which infall has been stopped for the time  $t_s$ , indicated on top of each dotted curve). The dashed line correspond to our detection limit.

already in the disk, and the galaxy is barely affected by the starvation process. Given the strong relationship between gas and star formation, the same conclusion applies to the  $H\alpha$  radial profile. Secondly, the resulting profiles never have the right shape, and never predict a sharp truncation, as is observed in all the short time-scale indicators (gas,  $H\alpha$ ,  $8\ \mu\text{m}$ ). While the models include a radial variation of infall time-scales (inside-out formation), this trend with galactocentric distance is not strong enough for the gas,  $H\alpha$  and FUV profiles to be truncated when infall is globally stopped at a given time.

The dependence of the infall time scale on the mass of the galaxy and on the radius are the ones encoded in the models. They would need to be dramatically changed in order to match the gas profile observed in NGC4569 in a starvation scenario. However, if the mass-dependence was extremely different, the models of Boissier & Prantzos (2000) would fail to reproduce other relations (e.g., the observed color magnitude relationship of nearby galaxies). The radial dependence of infall time-scales in these models is such that it provides a good match to the color and abundance gradients of spirals (Prantzos & Boissier 2000). This agreement would also be broken if we drastically changed this radial trend, as it would be needed to obtain a truncated profile, similar to the one observed in NGC4569.

#### 4.2. The ram pressure stripping scenario

Having such a simple prescription with only two free parameters (as explained in section 3.3), it is possible to choose simultaneously  $t_{rp}$  and  $\epsilon_0$  because the amount of gas left and its radial distribution depend strongly on  $\epsilon_0$  while the resulting stellar light profiles depend mainly on  $t_{rp}$  (see Fig.7 for some examples). If the time of cluster-core crossing is recent only the youngest stellar populations (emitting in  $H\alpha$ , whose age is  $\leq 4 \cdot 10^6$  yrs, or far-UV,  $\leq 10^8$  yrs) have had time to feel the progressive radial suppression of the star formation activity and we can date the suppression of gas with our model predictions. We stress that this model is principally constrained by the radial variation of the surface brightness and color profiles and only in a minor way by their absolute values which can be affected by zero-point uncertainties. Among the uncertainties, the extinction corrections are certainly the largest because the A(FUV) vs. TIR/FUV calibration is highly uncertain in such evolved galaxies where dust is not only heated by UV photons but also by the general interstellar radiation field produced by more evolved stars. Geometry and attenuation laws can vary from one galaxy to another; and without a complete radiative transfer model, it is impossible to apply “perfect” extinction corrections. We present in Figures 3 to 7 the data “as observed” (open symbols) and “extinction corrected” (filled symbols) in order to illustrate the sense and magnitude of the correction, and in doing so, illustrate just how much the uncertainty affects our results. It is obvious that allowing ourselves to change only two parameters ( $t_{rp}$  and  $\epsilon_0$ ) and considering the constraint of 16 profiles (total gas+photometry+rotation curve) does not result in a perfect match for all of them, especially taking into account the above-mentioned uncertainties. Models were computed each 100 Myr for  $0 < t_{rp} < 500$  Myr, 200 Myr for  $0.5 < t_{rp} < 1.5$  Gyr and 1 Gyr for  $1.5 < t_{rp} < 6.5$  Gyr; and in steps of  $0.2\ M_\odot\ \text{kpc}^{-2}\ \text{yr}^{-1}$  efficiencies between 0.4 and 1.6. Computing the  $\chi^2$  for various values of  $\epsilon_0$  and  $t_{rp}$  (see Fig. 8), we found that the model best matching the profiles of NGC 4569 is characterized by  $\epsilon_0 = 1.2\ M_\odot\ \text{kpc}^{-2}\ \text{yr}^{-1}$  and  $t_{rp} = 100$  Myr. The  $\chi^2$  for models with  $t_{rp} < 400$  Myr are still acceptable with  $\chi^2$  lower than 5 times the  $\chi^2$  of the best model ( $\chi^2_{min}=3.4$ ). The  $\chi^2$  for models in disagreement with observational limits at large radii (e.g. predicting too much gas or light in the outer disk where none is observed) are artificially set to large values to reject these solutions that cannot reproduce the observed truncations (shaded area in Fig. 8). Note that although the reduced  $\chi^2$  was computed, with 2 free parameters, the usual idea of a good fit ( $\chi^2 \sim 1$ ) cannot be achieved since we know that our models will not reproduce the small scale variations of the profiles (as mentioned above) and the introduction of observational limits makes any statistical analysis harder. In our study, the  $\chi^2$  is only used to pick out the best among the models, and see which parameters give similar results ( $t_{rp} < 400$  Myr), and which parameters produce very unrealistic models (large  $t_{rp}$  and low  $\epsilon_0$ ). For a few profiles Fig. 7 shows the observations contrasted with models of various ages ( $t_{rp}$ ) and of various efficiencies, showing that low and/or high efficiencies do not reproduce properly the gas and  $H\alpha$  truncation. In this figure, we also show a model with  $t_{rp} = 300$  Myr,

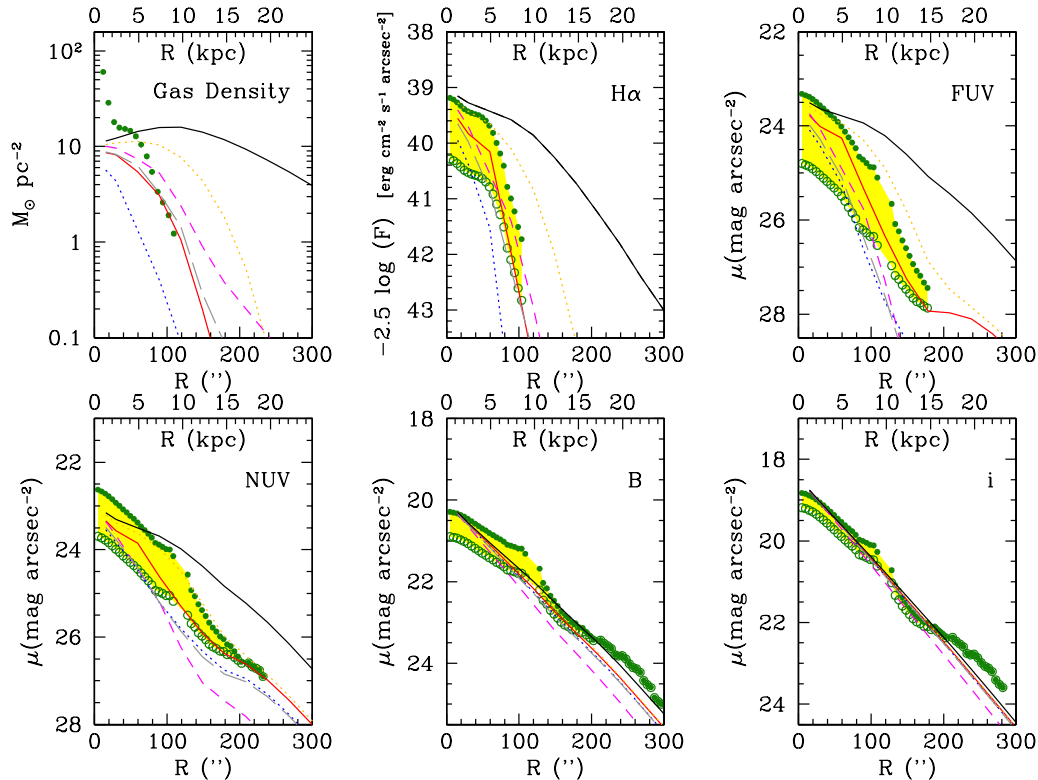


FIG. 7.— The radial profile of the observed (empty green circles) and extinction-corrected (filled green circles) total gas, H $\alpha$ , FUV (1530 Å), NUV (2310 Å), B and  $i$  surface brightness. The yellow shaded area marks the range in between the observed (bottom side) and extinction-corrected (top side) surface brightness profiles. Surface brightnesses are compared to the model predictions without interaction (black solid line) or with interaction (ram-pressure stripping) for several  $\epsilon_0$  and  $t_{rp}$  parameters. Equal maximum efficiency ( $\epsilon_0=1.2 M_\odot \text{ kpc}^{-2} \text{ yr}^{-1}$ ) and different age:  $t_{rp}=100$  Myr, red continuum line (the adopted model);  $t_{rp}=300$  Myr, grey long dashed line (time suggested by the Vollmer et al. 2004a study),  $t_{rp}=1.5$  Gyr, dashed magenta line. Equal age ( $t_{rp}=100$  Myr) and different maximum efficiency:  $\epsilon_0=3 M_\odot \text{ kpc}^{-2} \text{ yr}^{-1}$ , blue dotted line;  $\epsilon_0=1/3 M_\odot \text{ kpc}^{-2} \text{ yr}^{-1}$ , orange dotted line.

the time indicated by the dynamical model of Vollmer et al. (2004a). It is interesting to note that although earlier cluster-core-crossing epochs give more truncated disk profiles in the old stellar populations (B and  $i$  bands, blue dashed line), this is not the case in the gas profile which is modified by contributions from the recycled gas. Models with  $t_{rp} > 500$  Myr are quickly rejected because recycled gas from evolving stars would be present at large radii, thereby allowing some low levels of star formation. The model relative to the oldest interaction,  $t_{rp}=1.5$  Gyr given in Fig. 7 (dashed magenta line), predicts in fact a factor of  $\sim$  two higher total gas surface density outside the 80 arcsec radius than that observed.

This is largely consistent with the dynamical models of Vollmer et al. (2004a), who obtained  $t_{rp} \sim 300$  Myr, but do not reject shorter ( $\sim 100$  Myr) timescales (Vollmer, private communication). Although not reproducing perfectly the surface brightness profiles, the best-fitting model is able to qualitatively reproduce the truncation of the total gas disk profile and that of the H $\alpha$  and UV radial profiles, as well as the milder truncation observed at longer wavelengths (see Fig. 3). The comparison with the unperturbed model (assumed to represent an isolated spiral) clearly shows the effect of a ram-pressure-stripping event.

The ram-pressure model also reproduce (within the uncertainties) the radial trends of colors which are also clearly different from the unperturbed reference model. This is especially visible in Fig. 9 where we have compiled a few color profiles: the observed data (smoothed to match the model resolution), the unperturbed reference model, and the model including the perturbation. Color gradients at short wavelengths are inverted (redder colors outward) with respect to normal galaxies when gas removal is introduced into the model, as observed.

The adopted model does not take into account possible effects complicating the interaction. The most obvious one is the possibility for some of the gas to be re-accreted onto the galaxy following the stripping episode. This happens in several of the dynamical models run by Vollmer et al. (2001b). The effect is strongly dependent on the inclination angle of the galaxy with respect to its orbital plane, as well as the maximum ram pressure. In all of their models having a significant inclination (i.e., larger than 20 degrees), the re-accreted gas mass is lower than 10% of the stripped gas. If 10% of the stripped gas in our model was re-accreted (and distributed in a similar way to the gas profile we obtained), the gas profile would increase only by 0.4 dex, which would not be very different from the observed profiles. If we assume in

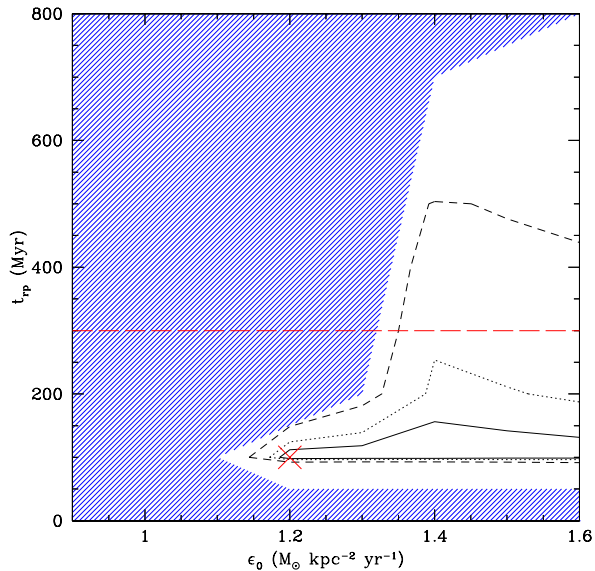


FIG. 8.— Reduced  $\chi^2$  as a function of the look-back time of the ram-pressure event  $t_{rp}$  and efficiency  $\epsilon_0$ . The contours (solid, dotted, dashed) show  $\chi^2$  levels of respectively  $2, 3, 5 \times \chi_{min}$  (the best model gives a value of  $\chi_{min} \sim 3.4$ ; a “perfect fit” with  $\chi^2 \sim 1$  cannot be achieved since the models will never reproduce observed small scales variations). The horizontal long-dashed line indicates the time suggested by the dynamical model of Vollmer et al. (2004a). The shaded area indicates values for which the model surface brightnesses are in disagreement with observational limits (non detections at relatively large radii). In this case, the  $\chi^2$  was arbitrarily given large values in order to reject these solutions that would not remove enough gas to properly reproduce the observed truncation.

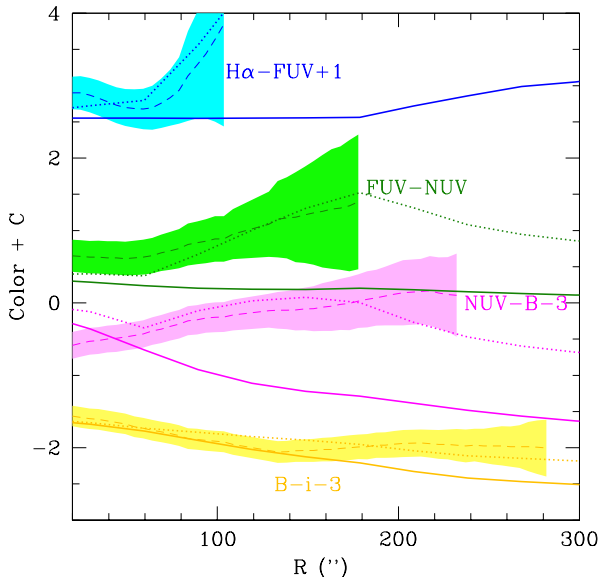


FIG. 9.— Observed color profile (dashed curve) and uncertainties (shaded area). The solid lines are the results of the unperturbed model, while the dotted lines correspond to the best-model with ram-pressure.

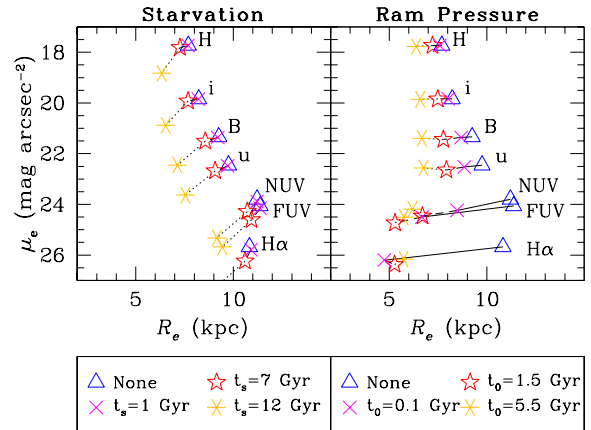


FIG. 10.— Variation of the effective surface brightness (mean surface brightness within  $R_e$ , the radius containing half of the total light) and radius due to differential variation of the star formation history of NGC 4569 in a) a starvation and b) ram-pressure stripping scenario. Open triangles are for the unperturbed model, the other symbols for different ages of the interaction.

the models that a much larger fraction of the gas (about 50%) is re-accreted, we would obtain HI column densities exceeding the observed ones. Another reason why we don’t expect much re-accretion to have taken place is that this phenomenon takes time: several 100 Myr years after the closest passage of the galaxy to the cluster center, a time similar to the look-back time we expect for this passage.

To conclude we can confidently say that the starvation scenario is very unlikely to have shaped the NGC4569 profiles, while the ram-pressure scenario is much more in agreement with the observations. With this scenario, we can exclude solutions older than  $\sim 500$  Myr, in agreement with the dynamical models of Vollmer et al.

## 5. DISCUSSION AND CONCLUSION

The present work gives the first quantitative estimate of the structural evolution of stellar disks in cluster galaxies due to gas removal caused by a dynamical interaction of the galaxy with the IGM, delivering a strong message concerning the passive stellar evolution of stripped disks. First of all it is clear that the truncation of the total gas disk profile is soon reflected on the young population stellar disk, confirming the predictions of Larson et al. (1980). As a consequence gas-stripped galaxies have color gradients opposite to that of normal, isolated spirals, which generally have bluer colors in their outer disks. NGC 4569 is bluest towards the center (see Fig. 9 and 11). The trend is especially true for colors tracing the relatively young populations ( $< \sim 10^8$  yr); colors tracing populations older than the interaction event show the usual gradient (i.e., redder towards the center, as the B-*i* color index). The inversion of the color gradient, here observed for the first time in a cluster galaxy, is well reproduced by our model.

The second major conclusion of the present analysis is that the perturbation which induced the truncation of the stellar disk of NGC 4569 is relatively recent event ( $\sim 100$  Myr, in any case  $\leq 500$  Myr). Ram-pressure is

avored with respect to starvation since the latter is simply not able to reproduce the observed truncation of the gas and star forming ( $H\alpha$ ,  $8\ \mu\text{m}$ , FUV) disk.

Since NGC 4569 seems to be typical of the HI-deficient galaxy population inhabiting nearby clusters, characterized by truncated HI and star forming disks (Cayatte et al. 1994; Koopmann et al. 2006), with largely unperturbed older stellar populations<sup>3</sup>, we generalize this statement by saying that gas stripping in cluster galaxies is due to relatively recent perturbations. This result is thus a major constraint on the evolution of cluster galaxies since it rejects long time-scale phenomena such as harassment and starvation.

The ram-pressure stripping scenario has recently been criticized as unable to reproduce the radial decrease with the cluster-centric distance of the star formation activity of galaxies in the nearby Universe. Recent, complete spectroscopic surveys of the nearby universe such as the SDSS or the 2dF have shown that the activity of late-type galaxies begins to decrease at 1-2 virial radii from the cluster center (Gomez et al. 2003; Lewis et al. 2002, Tanaka et al. 2004, Nichol 2004), scale-lengths comparable to those observed in the HI (Gavazzi et al. 2005, 2006a) and/or  $H\alpha$  (Gavazzi et al. 2002a, 2006b) in nearby clusters. Since these distances (1-2 virial radii) are significantly larger (a factor of 5-10) than those where galaxy-IGM interactions are expected to be more efficient ( $\sim$  inside a core radius), other processes already active at the periphery of clusters [such as galaxy harassment (Moore et al. 1996), starvation (Balogh et al. 2000) or pre-processing (Fujita 2004; Cortese et al. 2006b)] have been proposed to explain the radial decrease of the star formation activity with the cluster-centric distance.

As extensively discussed in Boselli & Gavazzi (2006), however, the presence of galaxies with clear signs of ongoing ram-pressure stripping at the periphery of nearby clusters and the large velocity dispersion, combined with the radial orbits (Dressler 1986; Solanes et al. 2001) of the late-type galaxy population can explain the observed decrease of the star forming activity at large cluster-centric radii in a ram-pressure stripping scenario. NGC 4569, for instance, might have travelled  $\sim 0.6$  Mpc ( $1/3$  of the virial radius) since it was stripped, a distance significantly larger than the core radius of the cluster (130 kpc). We recall that in Virgo the drop of the star formation in bright galaxies is observed at  $\sim 0.7$  virial radii (Gavazzi et al. 2006b), while the increase of the HI-deficiency parameter occurs at about 1 virial radius (Gavazzi et al. 2005). The higher velocity dispersion and IGM gas density of rich, evolved clusters, as well as a clumpy IGM distribution, might thus be at the origin of ram-pressure stripped galaxies up to  $\sim$  one virial radius.

One of the most intriguing (and still open) questions regarding the effects of the environment on the evolution of galaxies is that of the origin of lenticulars, and their overabundance in the centers of rich clusters. Are lenticulars an independent population of galaxies formed

in the primordial high-density environments, or were they spiral disks whose star formation activity had been quenched once their gas reservoir was removed by the unfavorable cluster environment? The present work has shown for the first time how a galaxy-cluster IGM interaction is able to remove most of the gas reservoir, inducing important structural modifications in the stellar disk properties. We have in fact shown that, because of the differential radial stellar evolution of spiral disks, we can expect that cluster spirals have (at least at short wavelengths) more truncated disk profiles, inverting the outer color gradient with respect to similar but unperturbed objects. The surface brightness of the disk, however, mildly decreases in  $H\alpha$  and in the UV bands while remaining mostly constant at longer wavelengths, even 5 Gyr after the interaction (Fig. 10)<sup>4</sup>. The differential evolution of the stellar disk due to gas stripping alone is thus not able to reproduce the  $\sim 0.65$  mag increased central surface brightness of present-day lenticulars (Dressler 1980; Boselli & Gavazzi 2006). In the case of starvation stellar disks are not truncated ( $R_e$  just slightly decreases) while surface brightnesses significantly decrease on long time scales.

Gravitational perturbations, such as tidal interactions with other galaxies (Merritt 1983), interactions with the cluster potential well (Byrd & Valtonen 1990) or a mixture of both must be invoked to reproduce the observed properties of nearby lenticulars. As described in the introduction, similar conclusions have been obtained from the analysis of statistical, kinematical, structural and spectro-photometrical properties of nearby clusters.

This new study is consistent with the idea that the present evolution of late-type galaxies in clusters differs from that at earlier epochs, where late-type galaxies were mostly perturbed by dynamical interactions (pre-processing and/or galaxy harassment; Dressler 2004, Moore et al. 1996) which were able to thicken the stellar disks thereby producing the present-day cluster lenticulars.

To conclude we can say that the combination of multifrequency observations of spatially resolved cluster galaxies combined with multi-zone spectro-photometric models of galaxy evolution provides an extremely useful tool to study the evolution of cluster galaxies. The results here presented for a typical HI-deficient, anemic Virgo cluster galaxy and extrapolated to the whole cluster galaxy population indicate that:

- 1) The gas removal due to a ram-pressure stripping event can reproduce the observed radial truncation of the stellar disk stronger at shorter wavelengths. On the other hand, starvation is not able to truncate gas or stellar disks.
- 2) As a consequence, color gradients make cluster objects redder in the outer disk than in the inner regions, and are thus inverted with respect to normal, isolated late-type galaxies.
- 3) This technique is useful to age-date the interaction. If NGC 4569 represents the typical HI-deficient cluster galaxy with truncated  $H\alpha$  and HI disk and normal intermediate age stellar disk, then our modeling suggests that

<sup>3</sup> We remind that there is a strong relationship between the ratio of the optical to  $H\alpha$  radii and the HI deficiency parameter in cluster galaxies (see Fig. 11 of Boselli & Gavazzi 2006).

<sup>4</sup> 40% of S0 galaxies in the Coma cluster underwent a star formation event in their centers in the last 5 Gyr, Poggianti et al. (2001).

gas stripping is a relatively recent event since it probably took place  $\leq 500$  Myr ago in these systems.

4) The effective surface brightness of the stripped galaxies remains constant or even mildly decreases after the interaction.

We hope to confirm this original result in the near future once multi-frequency data come available for a statistical significant sample of late-type cluster galaxies.

GALEX (Galaxy Evolution Explorer) is a NASA Small Explorer, launched in April 2003. We gratefully acknowl-

edge NASA's support for construction, operation, and science analysis for the GALEX mission, developed in cooperation with the Centre National d'Etudes Spatiales of France and the Korean Ministry of Science and Technology. We thank G. Gavazzi and N. Prantzos for their long-term collaboration in the subjects studied in this paper. S.B. thanks the CNES for its funding through GALEX-Marseille. We wish to thank B. Vollmer and J. Kenney for their valuable comments, and the GALEX SODA team for their help in the data reduction.

## REFERENCES

- Abazajian, K., et al., 2005, 129, 1755  
 Balogh, M.L., Navarro, J.F., & Morris, S.L., 2000, ApJ, 540, 113  
 Boissier, S., & Prantzos, N. 1999, MNRAS, 307, 857  
 Boissier, S. & Prantzos, N., 2000, MNRAS, 312, 398  
 Boissier, S., Boselli, A., Prantzos, N., & Gavazzi, G. 2001, MNRAS, 321, 733  
 Boissier, S., Prantzos, N., Boselli, A. & Gavazzi, G., 2003, MNRAS, 346, 1215  
 Boissier, S., Boselli, A., Buat, V., Donas, J. & Milliard, B., 2004, A&A, 424, 465  
 Boselli, A. & Gavazzi, G., 2002, A&A, 386, 124  
 Boselli, A. & Gavazzi, G., 2006, PASP, 118, 517  
 Boselli, A., Tuffs, R., Gavazzi, G., Hippelein, H. & Pierini, D., 1997, A&AS, 121, 507  
 Boselli, A., Gavazzi, G., Donas, J. & Scodreggio, M., 2001, AJ, 121, 753  
 Boselli, A., Lequeux, J. & Gavazzi, G., 2002, A&A, 384, 33  
 Boselli, A., Gavazzi, G. & Sanvito, G., 2003, A&A, 402, 37  
 Boselli, A., Lequeux, J., Gavazzi, G., 2004, A&A, 428, 409  
 Buat, V., Iglesias-Paramo, J., Seibert, M., et al., 2005, ApJ, 619, L51  
 Byrd, G. & Valtonen, M., 1990, ApJ, 350, 89  
 Cayatte, V., van Gorkom, J., Balkowski, C., & Kotanyi, C., 1990, AJ, 100, 604  
 Cayatte, V., Kotanyi, C., Balkowski, C. & van Gorkom, J., 1994, AJ, 107, 1003  
 Christlein, D., Zabludoff, A.I., 2004, ApJ, 616, 192  
 Cortese, L., Boselli, A., Buat, V., et al., 2006a, ApJ, 637, 242  
 Cortese, L., Gavazzi, G., Boselli, A., Franzetti, P., Kennicutt, R., O'Neil, K., Sakai, S., 2006b, A&A, in press (astro-ph/0603826)  
 Cowie, L.L., & Songaila, A., 1977, Nat., 266, 501  
 Dale, D., Helou, G., Contursi, A., Silberman, N., Kolhatkar, S., 2001, ApJ, 549, 215  
 Dale, D., Bendo, G., Engelbracht, C., et al., 2005, ApJ, 633, 857  
 Dressler, A., 1980, ApJ, 236, 351  
 Dressler, A., 1986, ApJ, 301, 85  
 Dressler, A., in "Clusters of Galaxies: Probes of Cosmological Structure and Galaxy Evolution", Cambridge University Press, ed. by Mulchaey et al., 2004, p. 207  
 Fujita, Y., 1998, ApJ, 509, 587  
 Fujita, Y., 2004, PASJ, 56, 29  
 Fujita, Y., Nagashima, M., 1999, ApJ, 516, 619  
 Gavazzi, G., Pierini, D. & Boselli, A., 1996, A&A, 312, 397  
 Gavazzi, G., Franzetti, P., Scodreggio, M., Boselli, A. & Pierini, D., 2000, A&A, 361, 863  
 Gavazzi, G., Boselli, A., Mayer, L., Iglesias-Paramo, J., Vilchez, J.M., Carrasco, L., 2001, ApJ, 563, L23  
 Gavazzi, G., Boselli, A., Pedotti, P., Gallazzi, A. & Carrasco, L., 2002a, A&A, 396, 449  
 Gavazzi, G., Bonfanti, C., Sanvito, G., Boselli, A., & Scodreggio, M., 2002b, ApJ, 576, 135  
 Gavazzi, G., Boselli, A., Donati, A., Franzetti, P. & Scodreggio, M., 2003, A&A, 400, 451  
 Gavazzi, G., Zaccardo, A., Sanvito, G., Boselli, A. & Bonfanti, C., 2004, A&A, 417, 499  
 Gavazzi, G., Boselli, A., van Driel, W., O'Neil, K., 2005, A&A, 429, 439  
 Gavazzi, G., O'Neil, K., Boselli, A., van Driel, W., 2006a, A&A, 449, 929  
 Gavazzi, G., Boselli, A., Cortese, L., Arosio, I., Gallazzi, A., Pedotti, P., Carrasco, L., 2006b, A&A, 443, 839  
 Gil de Paz, A. & Madore, B., 2005, ApJS, 156, 345  
 Gil de Paz, A., Boissier, S., Madore, B., et al., 2006, ApJS, in press  
 Gomez, P.L., Nichol, R.C., Miller, C.J., et al., 2003, ApJ, 584, 210  
 Gunn, J.E., & Gott, J.R.I., 1972, ApJ, 176, 1  
 Jarrett, T., Chester, T., Cutri, R., Schneider, S. & Huchra, J., 2003, AJ, 125, 525  
 Joglee, S., Scoville, N., Kenney, J., 2005, ApJ, 630, 837  
 Helfer, T., Thornley, M., Regan, M., et al., 2003, ApJS, 145, 259  
 Hinz, J.L., Rieke, G.H., & Caldwell, N., 2003, AJ, 126, 2622  
 Hou, J. L., Prantzos, N., & Boissier, S. 2000, A&A, 362, 921  
 Iglesias-Paramo, J., Boselli, A., Gavazzi, G., Zaccardo, A., 2004, A&A, 421, 887  
 Kenney, J. & Young, J., 1988, ApJS, 66, 261  
 Kenney, J., van Gorkom, J. & Vollmer, B., 2004, ApJ, 612, 127, 3361  
 Kennicutt, R., Armus, L., Bendo, G., et al., 2003, PASP, 115, 928  
 Koopmann, R. & Kenney, J., 2004a, ApJ, 613, 851  
 Koopmann, R. & Kenney, J., 2004b, ApJ, 613, 866  
 Koopmann, R., Haynes, M., Catinella, B., 2006, AJ, 131, 716  
 Kroupa, P., Tout, C. A., & Gilmore, G. 1993, MNRAS, 262, 545  
 Larson, R. B. 1976, MNRAS, 176, 31  
 Larson, R., Tinsley, B. & Caldwell, N., 1980, ApJ, 237, 692  
 Lewis, I., Balogh, M., De Propis, R., et al., 2002, MNRAS, 334, 673  
 Martin, C. L., & Kennicutt, R. C. 2001, ApJ, 555, 301  
 Merritt, D., 1983, ApJ, 264, 24  
 Mo, H. J., Mao, S., & White, S. D. M. 1998, MNRAS, 295, 319  
 Moore, B., Katz, N., Lake, G., Dressler, A. & Oemler, A., 1996, Nat., 379, 613  
 Nichol, R.C., 2004, in Clusters of Galaxies: Probes of Cosmological Structure and Galaxy Evolution, p24  
 Nulsen, P.E.J., 1982, MNRAS, 198, 1007  
 Poggianti, B.M., Bridges, T.J., Carter, D., et al., 2001, ApJ, 563, 118  
 Poggianti, B.M., Bridges, T.J., Komiyama, Y., et al., 2004, ApJ, 601, 197  
 Prantzos, N., & Boissier, S. 2000, MNRAS, 313, 338  
 Rubin, V., Waterman, A. & Kenney, J., 1999, AJ, 118, 236  
 Samland, M., Hensler, G., & Theis, C. 1997, ApJ, 476, 544  
 Solanes, J.M., Marricque, A., Garcia-Gomez, C., Gonzales-Casado, G., Giovanelli, R., Haynes, M., 2001, ApJ, 548, 97  
 Tanaka, M., Goto, T., Okamura, S., Shimasaku, K., & Brinkmann, J., 2004, AJ, 128, 2677  
 Tinsley, B. M. 1980, Fundamentals of Cosmic Physics, 5, 287  
 Treu, T., Ellis, R. S., Kneib, J.-P., Dressler, A., Smail, I., Czoske, O., Oemler, A., & Natarajan, P. 2003, ApJ, 591, 53  
 van den Bergh, S., 1976, ApJ, 206, 883  
 Vázquez, G. A., & Leitherer, C. 2005, ApJ, 621, 695  
 Vollmer, B., Cayatte, V., Boselli, A., Balkowski, C. & Duschl, W., 1999, A&A, 349, 411  
 Vollmer, B., Marcellin M., Amram, P., Balkowski, C., Cayatte, G., Garrido, O., 2000, A&A, 365, 532  
 Vollmer, B., Braine, J., Balkowski, C., Cayatte, V. & Duschl, W., 2001a, A&A, 374, 824  
 Vollmer, B., Cayatte, V., Balkowski, C. & Duschl, W., 2001b, ApJ, 561, 708  
 Vollmer, B., Balkowski, C., Cayatte, V., van Driel, W. & Huchtmeier, W., 2004a, A&A, 419, 35  
 Vollmer, B., Beck, R., Kenney, J., van Gorkom, J., 2004b, AJ, 127, 3375  
 Vollmer, B., Braine, J., Combes, F., Sofue, Y., 2005, A&A, 441, 473  
 Whitmore, B.C., Gilmore, D.M., & Jones, C., 1993, ApJ, 407, 489  
 Yoshida, M., Ohya, Y., Iye, M., et al., 2004, AJ, 127, 90

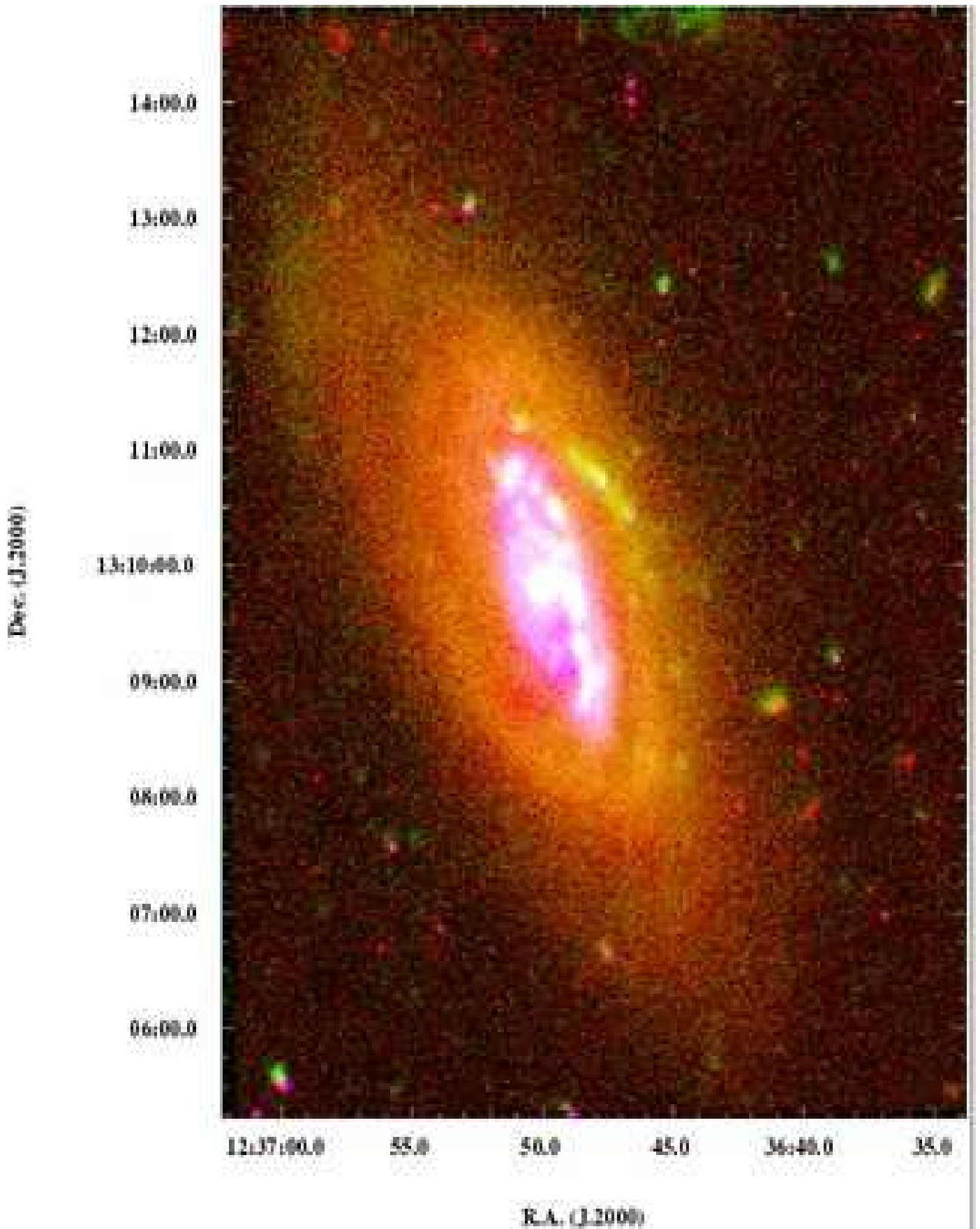


FIG. 11.— The RGB (continuum subtracted  $H\alpha$  =blue, FUV=green, red continuum near  $H\alpha$ =red) color map of NGC 4569. The NW spiral arm is visible at R.A.  $\sim 12^{\text{h}}37^{\text{m}}47^{\text{s}}$  and dec  $\sim 13^{\circ}10'40''$ .